Research Article

# ISP and PAP4 peptides promote motor functional recovery after peripheral nerve injury

https://doi.org/10.4103/1673-5374.294565

Date of submission: July 16, 2020

Date of decision: August 30, 2020

Date of acceptance: November 3, 2020

Date of web publication: January 7, 2021

Shi-Qin Lv[1], Wutian Wu[1, 2, *]

**Graphical Abstract** *Systemic treatment of PAP4 or ISP promotes axon regeneration and motor function recovery after spinal ventral root injury in adult rats*

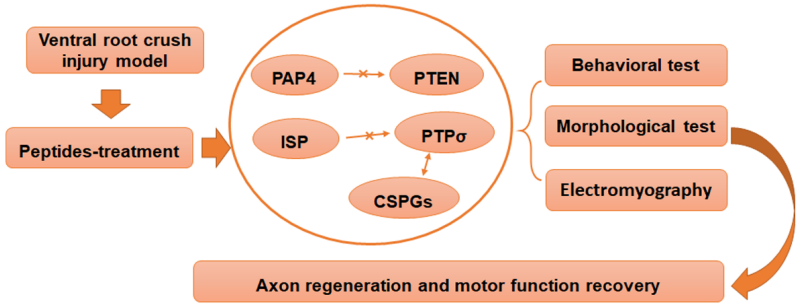


## Abstract

Both intracellular sigma peptide (ISP) and phosphatase and tensin homolog agonist protein (PAP4) promote nerve regeneration and motor functional recovery after spinal cord injury. However, the role of these two small peptides in peripheral nerve injury remains unclear. A rat model of brachial plexus injury was established by crush of the C6 ventral root. The rats were then treated with subcutaneous injection of PAP4 (497 μg/d, twice per day) or ISP (11 μg/d, once per day) near the injury site for 21 successive days. After ISP and PAP treatment, the survival of motoneurons was increased, the number of regenerated axons and neuromuscular junctions was increased, muscle atrophy was reduced, the electrical response of the motor units was enhanced and the motor function of the injured upper limbs was greatly improved in rats with brachial plexus injury. These findings suggest that ISP and PAP4 promote the recovery of motor function after peripheral nerve injury in rats. The animal care and experimental procedures were approved by the Laboratory Animal Ethics Committee of Jinan University of China (approval No. 20111008001) in 2011.

**Key Words:** axon; brachial plexus injury; crush injury; intracellular sigma peptide; motor function; PAP4; peripheral nerve; protection; regeneration; repair

Chinese Library Classification No. R453; R741; R722.14+4

## Introduction

Brachial plexus injury (BPI), a common chronic trauma, is characterized by severe motor dysfunction and permanent sensory impairment (Terzis et al., 2001). Various strategies have been used in an attempt to restore function and target innervation following injury (Carlstedt et al., 1995, 2020; Hoffmann et al., 1996; Fournier et al., 2001). However, effective therapies are lacking for this devastating injury because of the limited axon regrowth and inefficient target organ innervation (Navarro et al., 2007).

Studies indicate that the axonal outgrowth capacity of the peripheral nerve following injury largely depends on the combined action of multiple intrinsic and extrinsic factors (Allodi et al., 2012). Here, we focused on inhibiting chondroitin sulfate proteoglycans (CSPGs) and phosphatase and tensin homolog (PTEN). CSPG is the main component of transitional zone scar tissue, which acts as a barrier to axon regeneration. In the early stage of injury, astrocytes are activated and synthesize inhibitory CSPGs, which are secreted into the extracellular matrix, thereby impeding axonal outgrowth at the transitional zone (Yick et al., 2000; Silver and Miller, 2004). After the discovery of protein tyrosine phosphatase-σ (PTPσ), a neuronal receptor for CSPG, the underlying mechanism for CSPG inhibition was unearthed (Shen et al., 2009). It has been shown that modulating PTPσ can alleviate axonal growth inhibition by CSPGs and promote functional recovery following spinal cord injury (SCI), spinal root avulsion injury, dorsal root crush injury and ischemic heart attack (Gardner et al., 2015; Lang et al., 2015; Li et al., 2015; Yao et al., 2019). PTEN, a tumor suppressor that inhibits phosphoinositide 3-kinase/phospho-Akt signaling, plays a significant role in many physiological and pathological processes, including cellular growth, survival and metabolism (Zhou and Snider, 2006). Recent studies on neuronal PTEN inactivation, by either genetic or pharmacological means, have suggested

[1]Guangdong-Hong Kong-Macau Institute of CNS Regeneration, Ministry of Education CNS Regeneration Collaborative Joint Laboratory, Jinan University, Guangzhou, Guangdong Province, China; [2]Re-Stem Biotechnology Co., Ltd., Suzhou, Jiangsu Province, China

*Correspondence to: Wutian Wu, PhD, wtwu@hku.hk.

https://orcid.org/0000-0002-3662-9922 (Shi-Qin Lv)

***Funding:*** *This study was supported by the National Natural Science Foundation of China, No. 81971165; and the National Basic Research Program of China (973 Program), No. 2014CB542205 (both to WW).*

***How to cite this article:*** *Lv SQ, Wu W (2021) ISP and PAP4 peptides promote motor functional recovery after peripheral nerve injury. Neural Regen Res 16(8):1598-1605.*

that PTEN also plays an important role in neuroprotection and neuronal regeneration (Park et al., 2010; Ohtake et al., 2014). Substantial regrowth of lesioned corticospinal tract axons is induced in PTEN conditional knockout mice after SCI (Liu et al., 2010). In addition, PTEN blockade with bisperoxovanadium protects spinal cord tissues following SCI and enhances axon growth after sciatic nerve transection (Christie et al., 2010; Walker et al., 2012; Mao et al., 2013; Walker and Xu, 2014). Thus, modulating the intrinsic neuronal PTEN/mammalian target of the rapamycin pathway represents a potential strategy for promoting functional repair and axon regeneration following injury. However, genetic deletion of PTPσ or PTEN is not feasible for clinical treatment. In contrast, suppression by a pharmacological method allows control of initiation time, application period and drug dosage. Here, we investigate two small peptides, PTEN agonist protein (PAP4) and intracellular sigma peptide (ISP), as treatments for BPI. Among the five PAP proteins (PAP1–5), PAP4 is the most effective at reducing PTEN activity by targeting the C-terminal tail region (Ohtake et al., 2014). ISP is a small peptide mimic of the PTPσ wedge, which targets PTPσ and reduces the inhibitory effect of CSPG.

Although avulsion injury is a common animal model of BPI, axonal regeneration in this model exhibits considerable variability because of factors such as the site of surgical implantation, the interaction with the local environment and postoperative activity. Alternative models using nerve root crush can maintain central-peripheral nervous system connectivity, and thus are more stable and suitable for regeneration research than avulsion models (Carlstedt et al., 2000; Gu et al., 2004, 2005; Carlstedt, 2008; Spejo et al., 2013; Sakuma et al., 2016). Therefore, we employed a crush model at the proximal side of the C6 ventral root of rats and investigated the effects of both ISP and PAP4 on functional restoration following BPI.

## Materials and Methods

### Animals

Adult female Sprague-Dawley rats (8 weeks of age, weighing 230–250 g) were ordered from the Guangdong Medical Laboratory Animal Center (Foshan, China; license No. SCXK (Yue) 2018-0002). The animal care and experimental procedures were carried out according to the Laboratory Animal Ethics Committee guidelines at Jinan University (approval No. 20111008001) in 2011. Animals were housed under temperature-controlled conditions, with a normal 12/12-hour light/dark cycle and unrestricted access to water and food.

### Ventral spinal root crush injury model

Animal were anaesthetized with 1.0–2.0% isoflurane (RWD, Shenzhen, China). After opening the skin and removing connective tissue, the right lower cervical vertebra was exposed horizontally from the 4th cervical spine (C4) to the 7th cervical spine (C7) with a No. 15 scalpel. To more fully expose the right C5–7 dorsal root and open the dura, we removed the right vertebral lamina of C4–7 using a fine rongeur. The C5–7 dorsal roots were transected with ophthalmic scissors to better expose the ventral roots. We avulsed the C5 and C7 ventral roots using a fine glass hook without damaging the spinal cord (Su et al., 2013). The C6 ventral root was crushed three times (10 seconds per crush) with No. 7 forceps at the same site, with care taken to avoid rupture of the epineurium. After removing the C5 and C7 dorsal and ventral roots, we left the C6 ventral root as the sole connection between the spinal cord and biceps. The muscle and skin were sutured in layer after the surgery.

### Treatment and grouping

The preparation and application of PAP4 and ISP (both synthesized by CSBio, Shanghai, China) were empirically determined in previous work by Ohtake et al. (2014) and Li et al. (2015). Peptides were dissolved in dimethyl sulfoxide (20 mg/mL) and stored at –20°C before dilution to the required concentrations with phosphate-buffered saline (PBS) immediately prior to application. Rats with ventral spinal root crush injury were randomly divided into three groups and treated with PAP4, ISP or PBS. Briefly, rats received subcutaneous injections of PAP4 (497 μg/d, twice per day), ISP (11 μg/d, once a day) or PBS (0.5 mL/d) near the injury sight at 2 hours post-surgery for 21 consecutive days. All rats underwent behavioral, electrophysiological and morphological testing.

### Behavioral testing

#### *Terzis grooming test*

The Terzis grooming test (TGT) is widely used to assess motor functional recovery of an upper limb after surgical injury to rodents. Briefly, approximately 5 ml of water was sprayed onto the animal's head and snout, stimulating movement of the forelimbs to remove the water. Based on the position of the forepaw upon elbow flexion, a 0–5 scoring scale was used for upper limb injuries as follows: 0, no response; 1, flexion at elbow, not reaching the snout; 2, flexion at the elbow and forepaw able to reach the snout; 3, reaching higher than the snout, but below the eyes; 4, reaching to the eyes; 5, reaching to the ears and beyond (**Figure 1A**; Bertelli and Mira, 1993; Inciong et al., 2000). At 3 days post-surgery, the TGT was carried out and a score of 0 confirmed that the operation was successful. All animals were subjected to the TGT starting at the 3rd day after surgery, and repeated weekly from the day of surgery to the endpoint.

#### *Catwalk analysis*

The walking ability of injured animals was assessed and analyzed using the Catwalk system and EthoVision XT 9.0 software (Noldus, Leesburg, VA, USA). Footprint patterns, maximal contact area and the intensity of contact were recorded and measured by plotting the prints of the two front paws in one individual frame. At least three runs were required for each tested animal (Ding et al., 2014).

### Electromyography

The function of the biceps brachii was evaluated with electromyography (EMG). Briefly, at the terminal timepoint (3 weeks post-surgery), both left and right sides of the musculocutaneous nerve and biceps were exposed under Avertin (Macklin, Shanghai, China) anesthesia. After placing the bipolar stimulating electrode gently on the musculocutaneous nerve, we inserted the recording electrode into the center of the biceps and then two ground electrodes into the subcutaneous tissue. All tested animals ($n$ = 7 for the control group, $n$ = 6 each for the PAP4 and ISP groups) received the same stimulation (0.3 mA, 0.5 ms, 1 Hz) for 20 ms. EMG signals were collected with a multi-channel signal acquisition and processing system (RM6240BD; Chengdu Instrument Factory, Chengdu, China). At least three single responses on each bicep were measured at 2-minute intervals. The EMG amplitude of the evoked potentials was expressed as the right to left (R/L) ratio.

### Retrograde labeling and counting of labeled cells

At 3 weeks after ventral spinal root crush surgery, we randomly selected three to four animals in each group to undergo retrograde labeling experiments. Briefly, after euthanasia with 1.0–2.0% isoflurane (RWD), the right musculocutaneous nerve was exposed and slowly injected with approximately 0.8 μL of Fluorogold (Fluorochrome, 6% in sterilized water; AAT Bioquest Inc., Sunnyvale, CA, USA) at the same site under a surgical microscope (Leica, Wetzlar, Germany), and the labeled animals were perfused and fixed with 4% paraformaldehyde (Solarbio, Beijing, China) 4 days

after injection. After the dissection, spinal cord segments C5–7 were dehydrated in 30% sucrose for 2 days. Spinal cord segments were cut longitudinally at a thickness of 40 µm using a sliding microtome (Leica SM 2010R; Leica) following tissue processing. Observation and digitization were carried out under the fluorescence microscope (Carl Zeiss, Oberkochen, Germany) with a 405 nm filter. Labeled cells in the C5–7 segment were counted on every other section ($n$ = 4 for the PAP4 group, $n$ = 3 each for the ISP and control groups).

**Tissue preparation**

For histological staining, injured rats were euthanized by isoflurane, followed by intracardial perfusion with PBS and fixation with 4% paraformaldehyde at 3 weeks after crush surgery. The C5–7 spinal cord segments, musculocutaneous nerves and biceps brachii muscles were dissected and harvested for further analysis. The biceps muscles were weighed to evaluate the R/L weight ratio before the next processing step. After post fixation in 4% paraformaldehyde at 4°C for at least 2–4 hours, the tissue samples were dehydrated through a graded sucrose series (10%, 20%, 30%) for 24 hours each at 4°C. Then, cross sections of C5–7 spinal cord segments and the horizontal sections of biceps brachii were cut to 40 µm with a sliding microtome (Leica SM 2010R). Sections were stored in 24-well plates in PBS for histological staining. In addition, the musculocutaneous nerves were embedded with optimal cutting temperature compound and cut into cross sections at a thickness of 5 µm with a cryostat (Thermo Fisher Scientific, Waltham, MA, USA). All sections were used for staining.

**Assessment of motoneuron survival rate**

Every fourth section of the spinal C5–7 segment was utilized for choline acetyltransferase (ChAT) immunostaining. For antibody incubation, the sections were rinsed in PBS (3 × 5 minutes) and washed with 0.3% PBS-Triton-100 (3 × 15 minutes). Sections were incubated with ChAT antibody (1:500; Cat# AB144p, Millipore, Burlington, MA, USA) overnight at 4°C, followed by AlexaFluor 488-conjugated secondary antibody (1:1000; Cat# A11055, Thermo Fisher Scientific) for 2 hours at room temperature. The sections were mounted using anti-fade reagent with 4′,6-diamidino-2-phenylindole (Cat# P36935; Gibco, Thermo Fisher Scientific). Image acquisition was performed on a fluorescence microscope (Carl Zeiss) and ChAT-positive neurons on either side of the spinal anterior horn were counted with ImageJ (National Institutes of Health, Bethesda, MD, USA).

To confirm the immunofluorescence staining results, another series of slices was stained with 0.1% cresyl violet (Cat# G1430; Solarbio, Beijing, China) for 2 hours and dehydrated with ethanol. Images of Nissl-stained sections were captured with a light microscope (Olympus, Tokyo, Japan).

**Measurement of motor axons in the peripheral nerve**

The musculocutaneous nerve, 2 mm proximal to the biceps, was selected to provide standardized assessment of the number of motoneuron axons. Tissue processing was carried out as previously described, and 5-µm cross sections of the musculocutaneous nerve were incubated with neurofilament-200 (NF200; 1:500; Cat# N4142, Sigma, Burlington, MA, USA) as primary antibody and Alexa Fluor 594-conjugated donkey anti-rabbit IgG (1:1000; Cat# A21207, Thermo Fisher Scientific) as secondary antibody. The fluorescence microscope was used for image acquisition. Three slices were randomly selected from each tissue sample to count axon number.

Axonal diameters were measured using another series of musculocutaneous nerve slices stained with Luxol fast blue. The 5-µm cross sections were immersed in Luxol fast blue solution (Cat# DK0008, Leagene, Beijing, China) at 37°C for 20 hours, and then sequentially washed with 95% ethanol, water and 0.1% lithium carbonate (1–2 seconds). After washing the slices with water, the slides were sequentially dehydrated in 95% and 100% ethanol, rinsed in xylene twice and mounted under a coverslip using neutral balsam. Images were captured by a light microscope (Olympus). We randomly selected three slices for regenerated axonal diameter measurement, with ImageJ for data analysis.

**Examination of neuromuscular junctions**

Every fourth section of the biceps was used for neuromuscular junction (NMJ) analysis. The 40-µm sections from each animal were placed in different wells of a 24-well plate as described above. First, the sections were treated with 10 µg/mL proteinase k (Cat# P4850, Sigma) at 37°C for 10 minutes to expose the antigens. The sections were then incubated with NF200 antibody overnight at 4°C, followed by secondary antibody, as described above. The sections were thereafter stained with Alexa Fluor 488-conjugated α-bungarotoxin (1:500; Invitrogen) for 30 minutes. A fluorescence microscope was used for observation and image acquisition. The total number of NMJs in each series of slices from each bicep was used for comparison.

**Statistical analysis**

All statistical analyses were performed using GraphPad Prism 7.0 software (GraphPad, San Diego, CA, USA). Data are expressed as the mean ± standard error of the mean (SEM). One-way analysis of variance followed by the Tukey *post-hoc* test was used when more than two groups were compared. Two-way analysis of variance followed by the Bonferroni *post-hoc* test was used for comparing multiple groups at different timepoints. The significant difference level was set to 0.05.

## Results

**PAP4 and ISP promote motor functional recovery in rats with BPI**

Functional recovery is the ultimate aim in any therapy for BPI (Bertelli and Mira, 1993). Therefore, we used the TGT and catwalk analysis to investigate whether PAP4 and ISP can improve the motor function of the upper limb following spinal root crush injury. Before surgery, the upper limb of all animals was scored at 5, indicating normal elbow flexion. On the 3$^{rd}$ day after the operation, all animals underwent the TGT test with a score of 0, indicating complete loss of elbow flexion function. The recovery of elbow flexion started within 7 days after surgery in all three groups. The averaged TGT scores were considerably increased by PAP4 and ISP treatment at 14 (PAP4: $P$ = 0.0217; ISP: $P$ = 0.0026) and 21 days post-surgery (PAP4: $P$ = 0.0026; ISP: $P$ = 0.0002), compared with the control group (**Figure 1B**). The gait of injured rats was recorded and analyzed using Catwalk at 3 weeks post-surgery. By observing the three-dimensional prints, the paws and palms were clearly identified in the PAP4 and ISP groups, but not in the control group (**Figure 2A**). Furthermore, it was also easy to identify the palm and paws of the right forelimb in the PAP4 and ISP-treated groups from the two-dimensional footprints. By contrast, prints of the right forelimb in the control group were incomplete, although left forelimb prints were comparable to those in the treatment group (**Figure 2B**). We then measured the maximum contact area and the mean intensity as indicators of walking ability recovery. The mean intensity in the peptide-treated groups was significantly higher than that in the control (PAP4: $P$ = 0.0084; ISP: $P$ = 0.0156; **Figure 2C**). Compared with control rats, the maximum contact area in the PAP4 group was significantly greater ($P$ = 0.0010), but there was no significant difference between the control and ISP groups ($P$ = 0.0793; **Figure 2D**). These results indicate that both PAP4 and ISP promote functional motor recovery in rats after spinal root crush injury.

**PAP4 and ISP increase the number of surviving and regenerating motoneurons in the injured spinal cord segments of rats with BPI**

To determine whether PAP4 or ISP treatment can enhance the number of regenerating motoneurons after spinal root crush surgery, we performed retrograde labeling analysis by injecting FG solution into the distal musculocutaneous nerve and counted the numbers of Fluorogold-labeled cells in the spinal cord. We found that the mean number of Fluorogold-labeled cells in both the PAP4 and ISP groups was significantly higher than that in the control group (PAP4: $P$ = 0.0061; ISP: $P$ = 0.0200), suggesting that more motoneurons in peptide-treated animals projected their axons to the distal musculocutaneous nerve (**Figure 3A** and **B**). The results also suggest that the speed of axon regeneration was increased by peptide treatment. We also examined whether, in addition to accelerated regeneration, improved survival of motoneurons contributed to the increased number of retrogradely-labeled cells following PAP4 or ISP intervention. Three weeks after spinal root crush surgery, the right C5–7 spinal segment showed signs of shrinkage in all surgery groups. Because ChAT is a widely accepted marker of motoneurons (Hoang et al., 2003; Ohlsson et al., 2013), we used ChAT staining to assess motoneuron numbers to compare the survival rate of motoneurons between peptide-treated and control animals. In all groups, the numbers of motoneurons on the ipsilateral side were decreased compared with the contralateral side. The numbers of ChAT-positive neurons were higher in the PAP4 and ISP groups compared with the control group (PAP4: $P$ = 0.0402; ISP: $P$ = 0.0209; **Figure 3C** and **D**). We confirmed this result by Nissl staining. There were more surviving motoneurons in the PAP4 and ISP groups compared with the control group (PAP4: $P$ = 0.0473; ISP: $P$ = 0.0148; **Figure 3E** and **F**). These findings suggest that peptide treatment increases resilience to ongoing damage post-surgery.

**PAP4 and ISP increase the number and proportion of motor axons with greater diameter extending into the muscle after BPI**

Because the musculocutaneous nerve is an important conduit between spinal motoneurons and the biceps brachii, the number of regenerated axons is strongly related to the function of the injured upper limbs (Gu et al., 2004). Therefore, we next investigated whether PAP4 and ISP increase the number of motoneuron axons extending into the nerve trunk, using anti-NF200, 3 weeks after crush surgery. We found that the cross sections of the injured musculocutaneous nerve were inflated compared with the intact nerve. The number of NF200-positive axons on the intact side was higher compared with the injured side in all groups. However, the PAP4 and ISP groups had significantly more motoneurons compared with the control group (PAP4: $P$ = 0.0015; ISP: $P$ = 0.0002; **Figure 4A** and **C**). We further quantified the axonal diameter in the distal musculocutaneous nerve using Luxol fast blue staining 3 weeks after crush injury. Approximately 41% of axons in the control group fell into the diameter range of 1–2 μm, compared with 22% and 21% of PAP4 and ISP axons, respectively. Moreover, only about 4% of axonal diameters in the control group were larger than 5 μm, whereas over 19% and 18% of axonal diameters in the PAP4 and ISP-treated animals, respectively, were larger than 5 μm (0–1 μm: Control *vs*. PAP4: $P$ = 0.0573, Control *vs*. ISP: $P$ = 0.0437; 1–2 μm: Control *vs*. PAP4: $P$ < 0.0001, Control *vs*. ISP: $P$ < 0.0001; 4–5 μm: Control *vs*. PAP4: $P$ = 0.1262, Control *vs*. ISP: $P$ = 0.0247; > 5 μm: Control *vs.* PAP4: $P$ = 0.0022, Control *vs*. ISP: $P$ = 0.0028; **Figure 4B** and **D**). These results suggest that PAP4 and ISP greatly accelerate axon regeneration.

**PAP4 and ISP improve NMJ morphology and reduce muscle atrophy after BPI**

The recovery of motor function depends on regenerating motor axons successfully rebuilding synaptic connections with muscle fibers. The post-synaptic structure of NMJs features folds that increase connections with nerve fibers and is rich in acetylcholine receptors (Mills, 2005). After staining the nerve with NF200 and the muscle fibers with α-bungarotoxin, which specifically binds to acetylcholine receptors (Mills, 2005), we counted the total numbers of merged NMJs on every fourth section of bicep muscle. We found that the NMJs on the contralateral side had a normal size and shape, with strong connectivity between nerve and muscle, while the injured side displayed varying degrees of damage. In contrast, newly formed NMJs could be clearly observed in both PAP4 and ISP-treated animals (**Figure 5A**). Compared with the control group, the numbers of NMJs in the PAP4 ($P$ = 0.0323) and ISP groups ($P$ = 0.0076) were significantly higher (**Figure 5C**). To assess the extent of muscle atrophy, we also measured the wet weight of the biceps muscles 3 weeks after crush surgery. The wet weight ratios in the PAP4 and ISP groups were higher than those in control animals (PAP4: $P$ = 0.0021; ISP: $P$ = 0.0431; **Figure 5B** and **D**).

**PAP4 and ISP enhance EMG responses in rats with BPI**

Excitable motoneurons transmit and convey their orders to muscle fibers via electrical signals (Stålberg, 1991). Clinically, the health of motor units is detected by needle EMG, which measures extracellular electrical activity of muscle fibers. To evaluate whether the newly formed NMJs were functional, we recorded electromyograms from the biceps muscle after stimulating the musculocutaneous nerves 3 weeks after crush surgery. The EMG response to stimulation of the reinnervated muscles, particularly the peak-to-peak amplitude, was significantly greater in the PAP4 group (*vs*. Control: $P$ = 0.0387), but not significantly different between the control and ISP groups ($P$ = 0.0943) (**Figure 6B**). We also found that the EMG amplitude ratio in the PAP4 and ISP groups was higher than that in the control group (PAP4: $P$ = 0.0289; ISP: $P$ = 0.0245; **Figure 6C**).

## Discussion

Brachial plexus root injury often leads to neuronal death, axonal loss, atrophy of target organs and severe loss of motor function (Carlstedt, 2008). Although microsurgical interventions, such as nerve transfer, nerve grafts and artificial nerve conduit bridging have been widely performed to restore functional recovery and target innervation after BPI, the effectiveness of these surgical strategies remains poor, and consequently, the injured arm cannot regain normal movement (Hoffmann et al., 1993; Fournier et al., 2001; Gu et al., 2004; Hoang and Havton, 2006). It may be that the number of regenerating motoneurons projecting axons to the target organ is insufficient to achieve significant functional recovery. To develop better treatments for BPI, researchers have established a number of experimental animal models mimicking brachial plexus lesions that occur in patients, including spinal ventral root avulsion and crush.

Avulsion results in complete loss of connection between the motoneuron and its target, which usually interrupts neurotrophic factor anterograde transport, thereby causing neuronal death post-surgery (Koliatsos et al., 1994). In contrast, crush surgery retains the intact Schwann cell basal membrane surrounding the nerve fibers and preserves the pathway for the regenerating axon sprouts (Mazzer et al., 2008; Wong et al., 2011). Thus, compared with avulsion, spinal root crush seems to be a better axonotmetic animal model to evaluate the effect of pharmacological treatment.

Our results are consistent with previous studies showing that loss of neurons occurs following ventral root crush-approximately 40% of affected motoneurons died 3 weeks after crush injury, which may account for the limited effectiveness of certain surgical procedures (Spejo et al., 2013). Better strategies to accelerate axon regeneration after

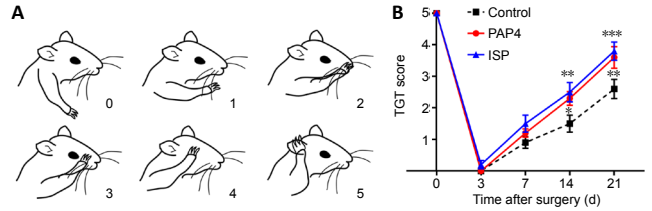


**Figure 1 | PAP4 and ISP treatments enhance recovery of elbow flexion after ventral spinal root surgery.**
(A) Positions of the forelimbs and corresponding scores (0–5) in the Terzis grooming test (TGT). (B) TGT scores pre- and post-surgery. Data are expressed as the mean ± SEM ($n$ = 10 in each group). *$P$ < 0.05, **$P$ < 0.01, ***$P$ < 0.001, *vs*. control group (two-way analysis of variance followed by the Bonferroni *post hoc* test). ISP: Intracellular sigma peptide; PAP4: phosphatase and tensin homolog agonist protein; TGT: Terzis grooming test.

spinal root injury are thus still required.

Recently, there has been increasing interest in pharmacological methods for neuroprotection and axon regeneration, particularly the application of small peptides, which presents an attractive and clinically feasible therapeutic option. With this in mind, this current study included multiple experiments examining the role of treatment with either one of two small peptides (ISP and PAP4) following spinal ventral root crush injury. We clearly demonstrated that both treatments markedly promote regeneration, resulting in increased survival of injured motoneurons, increased numbers of regenerated axons and healthier muscle units, ultimately leading to better functional recovery of the injured forelimb in comparison with vehicle treatment.

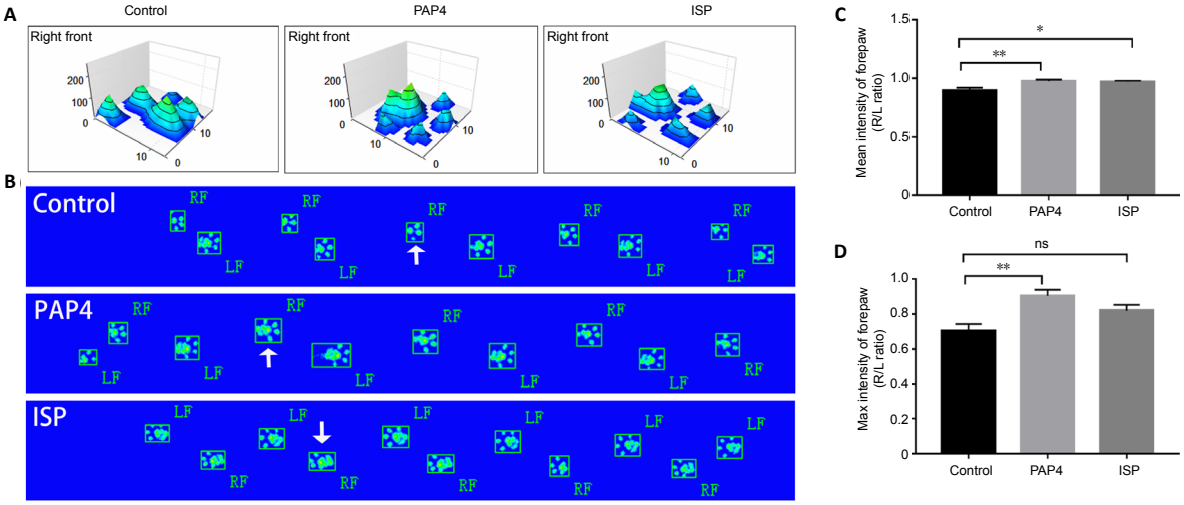


**Figure 2 | PAP4 and ISP treatments improve walking ability after ventral spinal root surgery.**
The Catwalk test was used to assess walking ability 3 weeks after surgery. (A) Three-dimensional footprint intensity charts of the lesion forelimb. PAP4 and ISP-treated animals showed clear prints of the palm and paws, whereas irregular prints were recorded from control animals. (B) Footprints of the upper limb. In PAP4 and ISP-treated animals, the footprints were fully identified. In control animals, the RF prints were incomplete, although the intact footprint (LF) was distinct. (C) Mean intensity of the forepaw. (D) Max contact area of the forepaw. Data are expressed as the mean ± SEM ($n$ = 14 in control group, $n$ = 12 in PAP4 group, $n$ = 11 in ISP group). *$P$ < 0.05, **$P$ < 0.01 (one-way analysis of variance followed by the Tukey *post hoc* test). ISP: Intracellular sigma peptide; L: left; LF: left forelimb; ns: not significant; PAP4: phosphatase and tensin homolog agonist protein; R: right; RF: right footprint.

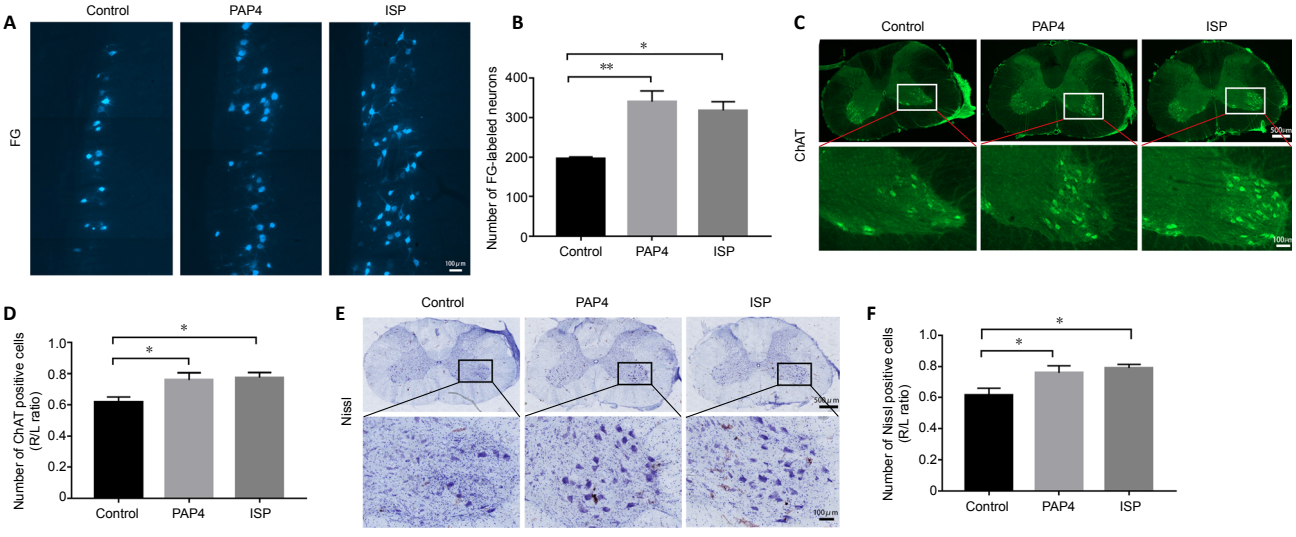


**Figure 3 | Motoneuron loss is reduced and regenerated motoneurons are increased after PAP4 and ISP treatments.**
(A) Representative images of FG-labeled cells. More labeled neurons were observed in PAP4 and ISP-treated rats. Scale bar: 100 μm. (B) Average FG-labeled cell number at 3 weeks post-surgery. (C) ChAT-positive cells (green: Alexa Fluor 488) in transversal sections. Scale bars: 500 μm (upper), 100 μm (lower). (D) Quantitative analysis of ChAT-positive cell number in the spinal cord. (E) Nissl staining of transverse sections of the spinal cord. Violet indicates Nissl-stained cells. Scale bars: 500 μm (upper), 100 μm (lower). (F) Quantitative analysis of Nissl-stained cells. Data are expressed as the mean ± SEM (B: $n$ = 4 in PAP4 group; $n$ = 3 in ISP and control groups; D, F: $n$ = 7 in each group). *$P$ < 0.05, **$P$ < 0.01 (one-way analysis of variance followed by the Tukey *post hoc* test). ChAT: Choline acetyltransferase; FG: Fluorogold; ISP: intracellular sigma peptide; L: left; PAP4: phosphatase and tensin homolog agonist protein; R: right.

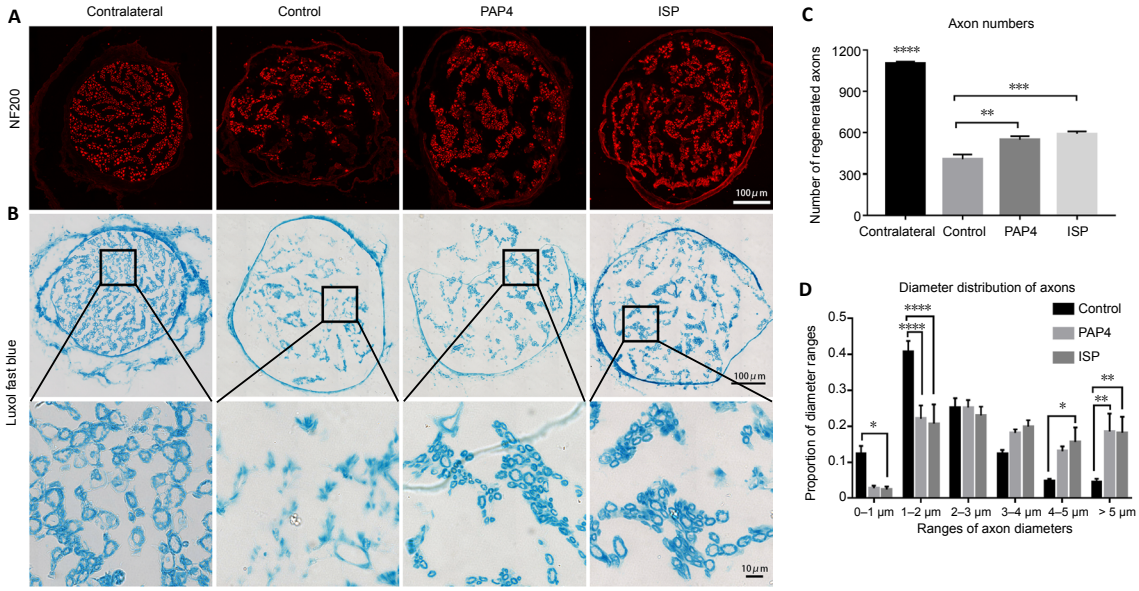


**Figure 4** | **Numbers of motoneuron axons are increased after PAP4 and ISP treatments.**
(A) Representative images of NF200-positive axons (red: Alexa Fluor 594) in cross sections of the distal musculocutaneous nerve at 3 weeks post-surgery. More axons were observed in both PAP4 and ISP-treated animals. Control animals showed fewer axons, the axons were more inflated, and the edge of the outer membrane was unclear. (B) Cross sections of the distal musculocutaneous nerve stained with Luxol fast blue. Both PAP4 and ISP-treated animals had more large-diameter axons, while control animals showed the opposite trend. Scale bars: 100 μm in A and upper row of B; 10 μm in lower row of B. (C) The number of axons in the distal musculocutaneous nerve. (D) Axonal size distribution in the distal musculocutaneous nerve 3 weeks after surgery. Data are expressed as the mean ± SEM (C: $n$ = 10 in contralateral; $n$ = 12 in PAP4 group; $n$ = 7 in control and ISP groups; D: $n$ = 5 in each group). *$P$ < 0.05, **$P$ < 0.01, ***$P$ < 0.001, ****$P$ < 0.0001 (two-way analysis of variance followed by the Bonferroni *post hoc* test). ISP: Intracellular sigma peptide; NF200: neurofilament-200; PAP4: phosphatase and tensin homolog agonist protein.

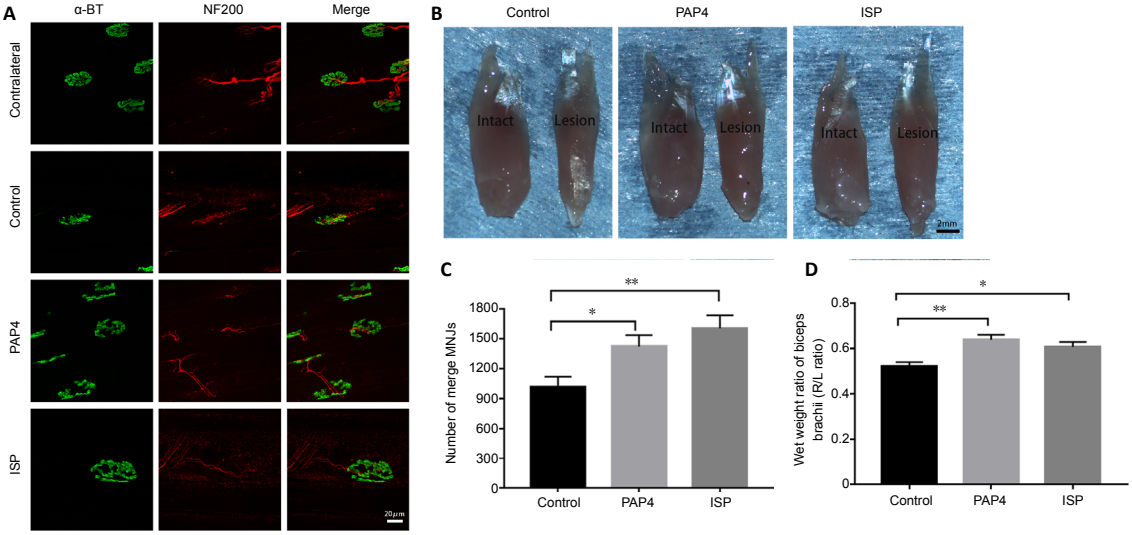


**Figure 5** | **PAP4 and ISP-treated animals have healthier neuromuscular junctions (NMJs) and reduced muscle atrophy.**
Three weeks after surgery, biceps were collected to study the number of neuromuscular junctions by α-BT and NF200 staining. (A) Representative images of α-BT (green: Alexa Fluor 488) and NF200-positive NMJs (red: Alexa Fluor 594). Compared with the lesion side, NMJs in the intact side showed a healthier morphology. (B) Three weeks post-surgery, left (intact side) and right (lesion side) biceps brachii were weighed. Compared with the intact side, the lesioned muscles showed severe atrophy. Scale bars: 20 μm in A, 2 mm in B. (C) Averaged number of NMJs in the biceps. (D) The wet weight ratio of the biceps brachii. Data are expressed as the mean ± SEM (C: $n$ = 12 in control group; n = 13 in PAP4 group; $n$ = 7 in ISP group; D: $n$ = 12 in PAP4 group; $n$ = 8 in control and ISP groups). *$P$ < 0.05, **$P$ < 0.01 (one-way analysis of variance followed by the Tukey's *post hoc* test). α-BT: α-Bungarotoxin; ISP: intracellular sigma peptide; L: left; NF200: neurofilament-200; PAP4: phosphatase and tensin homolog agonist protein; R: right.

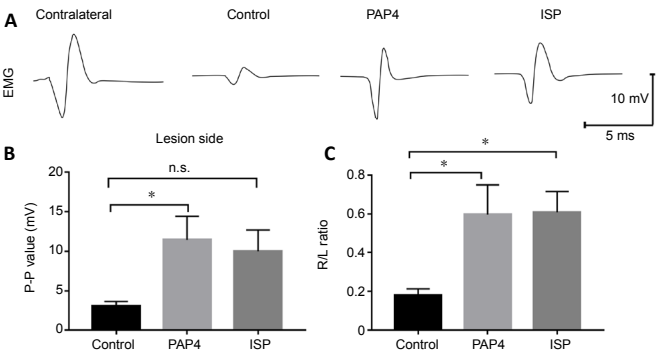


**Figure 6** | **EMG amplitude in re-innervated muscles is higher in PAP4 and ISP-treated animals than in control animals.**
EMG recording of musculocutaneous nerve stimulation in the biceps 3 weeks post-operation. (A) Representative images of EMG amplitude in the intact side (contralateral) and the lesion side of control, PAP4 and ISP animals. On the lesion sides, the P-P value is reduced in control rats. (B) Averaged P-P value in the lesion side. (c) EMG amplitude. Data are expressed as the mean ± SEM ($n$ = 7 in control group and $n$ = 6 in PAP4 and ISP groups). *$P$ < 0.05 (one-way analysis of variance followed by the Tukey's *post hoc* test). EMG: Electromyography; ISP: intracellular sigma peptide; L: left; n.s.: not significant; PAP4: phosphatase and tensin homolog agonist protein; P-P: peak-to-peak amplitude; R: right.

As mentioned before, severe progressive neuronal death after spinal ventral root injury is the main obstacle to recovery (Wu and Li, 1993; Eggers et al., 2010). Therefore, increasing the survival rate of injured motoneurons is a prerequisite for the regeneration of axons. We demonstrated that treatment with ISP increased motoneuron survival rate compared with the control group, from 61% to 79%, at 3 weeks after spinal ventral root crush injury by overcoming the regeneration barrier. Our results support previous studies demonstrating ISP treatment achieves a motoneuron survival rate of 80% at 12 weeks following avulsion injury (Li et al., 2015). We also demonstrated that treatment with PAP4, the other small peptide in our study, significantly improved motoneuron survival. This is most likely due to inhibition of PTEN. Indeed, it has been reported that PTEN-deficient dopamine neurons transplanted into Parkinson's disease mouse models are less susceptible to cell death and extend longer axons than control grafts (Zhang et al., 2012). Because PTEN appears to be important in restricting mature neuron regeneration, inactivation of this pathway may also have therapeutic potential for other neuronal disorders characterized by axonal damage.

Although peripheral nerve fibers have considerable potential for self-regeneration, the outcome following significant injury is often unsatisfactory. It is reported that both intrinsic regrowth capability and extracellular environment determine the outcome of regeneration. After injury, activated astrocytes synthesize and release inhibitory CSPGs that can persist for months, blocking axon elongation (Fraher, 2000; Silver and Miller, 2004; Cregg et al., 2014). In fact, modulation of PTPσ to achieve CSPG inhibition enhances functional recovery and axonal regeneration in both SCI and spinal root avulsion models (Lang et al., 2015; Li et al., 2015). In the present study, using ISP to achieve CSPG inhibition, we found that the number of axons in the proximal site of the musculocutaneous nerve was markedly higher than that in the control group. PTEN also plays a critical role in modulating axon formation and extension. Recent studies on neuronal PTEN inactivation by transgenic deletion or pharmacological inhibition demonstrate enhanced regeneration of lesioned central and peripheral nervous system axons (Ohtake et al., 2015). After SCI, systemic PAP treatments by subcutaneous delivery stimulate the regrowth of descending serotonergic axons in the caudal spinal cord of adult mice with dorsal hemisection at T7. Systemic PAP treatment also promotes corticospinal tract axon rostral sprouting towards the lesion and inhibits corticospinal tract axon regrowth in the caudal spinal cord (Ohtake et al., 2014). However, evidence that PAPs play a positive role in the peripheral nervous system was lacking. Our work here demonstrates that the number of regenerating axons can be greatly increased by PAP4 intervention. Furthermore, by Luxol fast blue staining, we found that axons in both PAP4 and ISP-treated animals were larger than those in the control group. These results indicate that there are more regenerated axons of a larger size after systemic treatment with PAP4 or ISP.

The greater number of motor axons regenerated from motoneurons in the peptide-treated groups likely promotes the rebuilding of synapses with the NMJ. Indeed, our results here show that peptide therapy positively influences target re-innervation. Animals that received ISP or PAP4 treatment not only showed a significant reduction in NMJ detachment and muscle atrophy, but also a remarkable increase in neuromuscular electrophysiological activity. Importantly, systemic ISP and PAP4 promoted locomotor functional recovery 3 weeks following spinal ventral root crush injury, demonstrated by increased TGT scores and intensity of forelimb walking and clear footprints. In summary, our current findings show that both ISP and PAP4 represent promising options for the treatment of spinal root injuries. However, our study lacks evidence from in vitro experiments. Moreover, the complex mechanisms underlying the therapeutic effectiveness of systemic ISP and PAP4 application will require further study to clarify.

**Author contributions:** *Study conception and design: WW; experiment implementation and data collection: SQL; manuscript writing and figure preparation: SQL, WW. Both authors approved the final version of the manuscript.*
**Conflicts of interest:** *WW was employed by Re-Stem Biotechnology Co., Ltd., Suzhou, China. The authors declare no competing interests.*
**Financial support:** *This study was supported by the National Natural Science Foundation of China, No. 81971165; and the National Basic Research Program of China (973 Program), No. 2014CB542205 (both to WW). The funding sources had no role in study conception and design, data analysis or interpretation, paper writing or deciding to submit this paper for publication.*
**Institutional review board statement:** *The study was approved by the Laboratory Animal Ethics Committee of Jinan University, China (approval No. 20111008001) in 2011.*
**Copyright license agreement:** *The Copyright License Agreement has been signed by both authors before publication.*
**Data sharing statement:** *Datasets analyzed during the current study are available from the corresponding author on reasonable request.*
**Plagiarism check:** *Checked twice by iThenticate.*
**Peer review:** *Externally peer reviewed.*

**Open peer reviewers:** *Renata Ciccarelli, University of Chieti-Pescara, Italy; Emily Burnside, King's College London, UK.*
**Additional files:**
***Additional file 1:*** *Open peer review reports 1 and 2.*
***Additional file 2:*** *Original data of the experiment.*

## References

Allodi I, Udina E, Navarro X (2012) Specificity of peripheral nerve regeneration: interactions at the axon level. Prog Neurobiol 98:16-37.

Bertelli JA, Mira JC (1993) Behavioral evaluating methods in the objective clinical assessment of motor function after experimental brachial plexus reconstruction in the rat. J Neurosci Methods 46:203-208.

Carlstedt T (2008) Root repair review: basic science background and clinical outcome. Restor Neurol Neurosci 26:225-241.

Carlstedt T, Grane P, Hallin RG, Norén G (1995) Return of function after spinal cord implantation of avulsed spinal nerve roots. Lancet 346:1323-1325.

Carlstedt T, Anand P, Hallin R, Misra PV, Norén G, Seferlis T (2000) Spinal nerve root repair and reimplantation of avulsed ventral roots into the spinal cord after brachial plexus injury. J Neurosurg 93:237-247.

Christie KJ, Webber CA, Martinez JA, Singh B, Zochodne DW (2010) PTEN inhibition to facilitate intrinsic regenerative outgrowth of adult peripheral axons. J Neurosci 30:9306-9315.

Cregg JM, DePaul MA, Filous AR, Lang BT, Tran A, Silver J (2014) Functional regeneration beyond the glial scar. Exp Neurol 253:197-207.

Ding Y, Qu Y, Feng J, Wang M, Han Q, So KF, Wu W, Zhou L (2014) Functional motor recovery from motoneuron axotomy is compromised in mice with defective corticospinal projections. PLoS One 9:e101918.

Eggers R, Tannemaat MR, Ehlert EM, Verhaagen J (2010) A spatio-temporal analysis of motoneuron survival, axonal regeneration and neurotrophic factor expression after lumbar ventral root avulsion and implantation. Exp Neurol 223:207-220.

Fournier HD, Menei P, Khalifa R, Mercier P (2001) Ideal intraspinal implantation site for the repair of ventral root avulsion after brachial plexus injury in humans. A preliminary anatomical study. Surg Radiol Anat 23:191-195.

Fraher JP (2000) The transitional zone and CNS regeneration. J Anat 196:137-158.
Gardner RT, Wang L, Lang BT, Cregg JM, Dunbar CL, Woodward WR, Silver J, Ripplinger CM, Habecker BA (2015) Targeting protein tyrosine phosphatase σ after myocardial infarction restores cardiac sympathetic innervation and prevents arrhythmias. Nat Commun 6:6235.
Gu HY, Chai H, Zhang JY, Yao ZB, Zhou LH, Wong WM, Bruce I, Wu WT (2004) Survival, regeneration and functional recovery of motoneurons in adult rats by reimplantation of ventral root following spinal root avulsion. Eur J Neurosci 19:2123-2131.
Gu HY, Chai H, Zhang JY, Yao ZB, Zhou LH, Wong WM, Bruce IC, Wu WT (2005) Survival, regeneration and functional recovery of motoneurons after delayed reimplantation of avulsed spinal root in adult rat. Exp Neurol 192:89-99.
Hoang TX, Havton LA (2006) A single re-implanted ventral root exerts neurotropic effects over multiple spinal cord segments in the adult rat. Exp Brain Res 169:208-217.
Hoang TX, Nieto JH, Tillakaratne NJ, Havton LA (2003) Autonomic and motor neuron death is progressive and parallel in a lumbosacral ventral root avulsion model of cauda equina injury. J Comp Neurol 467:477-486.
Hoffmann CF, Thomeer RT, Marani E (1993) Reimplantation of ventral rootlets into the cervical spinal cord after their avulsion: an anterior surgical approach. Clin Neurol Neurosurg 95 Suppl:S112-118.
Hoffmann CF, Marani E, van Dijk JG, vd Kamp W, Thomeer RT (1996) Reinnervation of avulsed and reimplanted ventral rootlets in the cervical spinal cord of the cat. J Neurosurg 84:234-243.
Inciong JG, Marrocco WC, Terzis JK (2000) Efficacy of intervention strategies in a brachial plexus global avulsion model in the rat. Plast Reconstr Surg 105:2059-2071.
Koliatsos VE, Price WL, Pardo CA, Price DL (1994) Ventral root avulsion: an experimental model of death of adult motor neurons. J Comp Neurol 342:35-44.
Lang BT, Cregg JM, DePaul MA, Tran AP, Xu K, Dyck SM, Madalena KM, Brown BP, Weng YL, Li S, Karimi-Abdolrezaee S, Busch SA, Shen Y, Silver J (2015) Modulation of the proteoglycan receptor PTPσ promotes recovery after spinal cord injury. Nature 518:404-408.
Li H, Wong C, Li W, Ruven C, He L, Wu X, Lang BT, Silver J, Wu W (2015) Enhanced regeneration and functional recovery after spinal root avulsion by manipulation of the proteoglycan receptor PTPσ. Sci Rep 5:14923.
Liu K, Lu Y, Lee JK, Samara R, Willenberg R, Sears-Kraxberger I, Tedeschi A, Park KK, Jin D, Cai B, Xu B, Connolly L, Steward O, Zheng B, He Z (2010) PTEN deletion enhances the regenerative ability of adult corticospinal neurons. Nat Neurosci 13:1075-1081.
Mao L, Jia J, Zhou X, Xiao Y, Wang Y, Mao X, Zhen X, Guan Y, Alkayed NJ, Cheng J (2013) Delayed administration of a PTEN inhibitor BPV improves functional recovery after experimental stroke. Neuroscience 231:272-281.
Mazzer PY, Barbieri CH, Mazzer N, Fazan VP (2008) Morphologic and morphometric evaluation of experimental acute crush injuries of the sciatic nerve of rats. J Neurosci Methods 173:249-258.
Mills KR (2005) The basics of electromyography. J Neurol Neurosurg Psychiatry 76 Suppl 2:ii32-35.
Navarro X, Vivó M, Valero-Cabré A (2007) Neural plasticity after peripheral nerve injury and regeneration. Prog Neurobiol 82:163-201.
Ohlsson M, Nieto JH, Christe KL, Havton LA (2013) Long-term effects of a lumbosacral ventral root avulsion injury on axotomized motor neurons and avulsed ventral roots in a non-human primate model of cauda equina injury. Neuroscience 250:129-139.
Ohtake Y, Hayat U, Li S (2015) PTEN inhibition and axon regeneration and neural repair. Neural Regen Res 10:1363-1368.
Ohtake Y, Park D, Abdul-Muneer PM, Li H, Xu B, Sharma K, Smith GM, Selzer ME, Li S (2014) The effect of systemic PTEN antagonist peptides on axon growth and functional recovery after spinal cord injury. Biomaterials 35:4610-4626.
Park KK, Liu K, Hu Y, Kanter JL, He Z (2010) PTEN/mTOR and axon regeneration. Exp Neurol 223:45-50.
Sakuma M, Gorski G, Sheu SH, Lee S, Barrett LB, Singh B, Omura T, Latremoliere A, Woolf CJ (2016) Lack of motor recovery after prolonged denervation of the neuromuscular junction is not due to regenerative failure. Eur J Neurosci 43:451-462.
Shen Y, Tenney AP, Busch SA, Horn KP, Cuascut FX, Liu K, He Z, Silver J, Flanagan JG (2009) PTPsigma is a receptor for chondroitin sulfate proteoglycan, an inhibitor of neural regeneration. Science 326:592-596.
Silver J, Miller JH (2004) Regeneration beyond the glial scar. Nat Rev Neurosci 5:146-156.
Spejo AB, Carvalho JL, Goes AM, Oliveira AL (2013) Neuroprotective effects of mesenchymal stem cells on spinal motoneurons following ventral root axotomy: synapse stability and axonal regeneration. Neuroscience 250:715-732.
Stålberg E (1991) Invited review: electrodiagnostic assessment and monitoring of motor unit changes in disease. Muscle Nerve 14:293-303.
Su H, Yuan Q, Qin D, Yang X, Wong WM, So KF, Wu W (2013) Ventral root re-implantation is better than peripheral nerve transplantation for motoneuron survival and regeneration after spinal root avulsion injury. BMC Surg 13:21.
Terzis JK, Vekris MD, Soucacos PN (2001) Brachial plexus root avulsions. World J Surg 25:1049-1061.
Walker CL, Xu XM (2014) PTEN inhibitor bisperoxovanadium protects oligodendrocytes and myelin and prevents neuronal atrophy in adult rats following cervical hemicontusive spinal cord injury. Neurosci Lett 573:64-68.
Walker CL, Walker MJ, Liu NK, Risberg EC, Gao X, Chen J, Xu XM (2012) Systemic bisperoxovanadium activates Akt/mTOR, reduces autophagy, and enhances recovery following cervical spinal cord injury. PLoS One 7:e30012.
Wong KH, Naidu M, David P, Abdulla MA, Abdullah N, Kuppusamy UR, Sabaratnam V (2011) Peripheral nerve regeneration following crush injury to rat peroneal nerve by aqueous extract of medicinal mushroom Hericium erinaceus (Bull.: Fr) Pers. (Aphyllophoromycetideae). Evid Based Complement Alternat Med 2011:580752.
Wu W, Li L (1993) Inhibition of nitric oxide synthase reduces motoneuron death due to spinal root avulsion. Neurosci Lett 153:121-124.
Yao M, Sun H, Yuan Q, Li N, Li H, Tang Y, Leung GK, Wu W (2019) Targeting proteoglycan receptor PTPσ restores sensory function after spinal cord dorsal root injury by activation of Erks/CREB signaling pathway. Neuropharmacology 144:208-218.
Yick LW, Wu W, So KF, Yip HK, Shum DK (2000) Chondroitinase ABC promotes axonal regeneration of Clarke's neurons after spinal cord injury. Neuroreport 11:1063-1067.
Zhang Y, Granholm AC, Huh K, Shan L, Diaz-Ruiz O, Malik N, Olson L, Hoffer BJ, Lupica CR, Hoffman AF, Bäckman CM (2012) PTEN deletion enhances survival, neurite outgrowth and function of dopamine neuron grafts to MitoPark mice. Brain 135:2736-2749.
Zhou FQ, Snider WD (2006) Intracellular control of developmental and regenerative axon growth. Philos Trans R Soc Lond B Biol Sci 361:1575-1592.

*P-Reviewers: Ciccarelli R, Burnside E; C-Editor: Zhao M; S-Editors: Yu J, Li CH; L-Editors: Patel B, Yu J, Song CP; T-Editor: Jia Y*